ACTA ABP BIOCHIMICA POLONICA

Vol. 69, No 4/2022
767–772
https://doi.org/10.18388/abp.2020_6021

Regular paper

# Circ_FOXO3 regulates KLF6 through sponge adsorption of miR-122-5p to repress $H_2O_2$-induced HBVSMC proliferation, thus promoting IA development *in vitro* model

Pei Dong Yue, Ya Nan Lu, Lei Zhang and Zheng Fei Ma✉

Department of Neurosurgery, Suzhou Hospital of Anhui Medical University (Suzhou Municipal Hospital of Anhui Province), SuZhou City, AnHui Province, 234000, China

**Purpose: The phenotypic transformation of human brain vascular smooth muscle cells (HBVSMC) is widely involved in the appearance and progression of intracranial aneurysms (IA). Aneurysm (IA) Circular RNA circ_FOXO3 functions pivotally in vascular diseases and tumors, but its regulatory role as well as its molecular mechanism in IA is still uncertain. This research was to explore how circ_FOXO3 works and its mechanism *in vitro* model of HBVSMC IA induced by $H_2O_2$. Methods: Thirty-eight patients with IA and their normal tissues were clinically collected. Examination of endothelin-1, vascular hematoma factor, circ_FOXO3, microRNA (miR)-122-5p and KLF6 and the correlation of circ_FOXO3 with clinical case information were ensured. Establishment of an *in vitro* IA model was through HBVSMC induced by $H_2O_2$ and transfection with circ_FOXO3, miR-122-5p and KLF6 related plasmids was to figure out their roles in cell growth. The relationship among circ_FOXO3, miR-122-5p with KLF6 was detected. Results: Up-regulated circ_FOXO3 and KLF6 and reduced miR-122-5p were in IA tissues; Circ_FOXO3 was associated with smoking history, Hunt-Hess grading and endothelial injury degree. Repressive circ_FOXO3 or KLF6 and strengthening miR-122-5p facilitated $H_2O_2$-induced proliferation and repressed HBVSMC apoptosis, while elevation of circ_FOXO3 or depressive miR-122-5p was opposite. circ_FOXO3 bound to miR-122-5p, whose target was KLF6, which participated in controlling IA by mediating the circ_FOXO3/miR-122-5p axis. Conclusion: In summary, the findings suggest that circ_FOXO3 suppresses $H_2O_2$-induced proliferation of HBVSMC but promotes apoptosis *via* modulation of miR-122-5p/KLF6 axis. Targeted therapy of circ_FOXO3/miR-122-5p/KLF6 axis is supposed to be a promising treatment approach for IA patients.**

**Keywords**: circular RNA circ_FOXO3; microRNA-122-5p; Promote; Intracranial aneurysm

**Received**: 12 November, 2021; revised: 23 December, 2021; accepted: 18 March, 2022; available on-line: 22 October, 2022

✉e-mail: mazfei817@hotmail.com

**Abbreviations**: circRNAs, circular RNAs; IA, intracranial aneurysm; miRNAs, microRNAs; ncRNAs, noncoding RNAs; VSMC, vascular smooth muscle cells

## INTRODUCTION

Intracranial aneurysm (IA) is a serious cerebral vascular degeneration that often leads to fatal vessel rupture and subarachnoid hemorrhage (Maumus-Robert *et al.,* 2020) . Despite decades of research, effective treatments for IA are still limited (Etminan *et al.,* 2016). The molecular basis for the formation and rupture of IA is complex and the dysfunction of vascular smooth muscle cells (VSMC) is related to the pathogenesis of IA (Mandelbaum *et al.,* 2013; Frösen *et al.,* 2018). VSMC apoptosis can lead to vascular wall degradation, thus inducing the occurrence and rupture of IA (Liu *et al.,* 2019). Therefore, exploring the mechanisms of proliferation and apoptosis of VSMC is helpful to find a new way to treat IA. Circular RNAs (circRNAs) are noncoding RNAs (ncRNAs) formed by covalently closed loops that are widely expressed in human cells (Salzman *et al.,* 2012). In recent years, with the wide application of RNA sequencing technology, it has been found that many exon transcripts can accept nonlinear reverse splicing or gene rearrangement to form circRNAs (Chen *et al.,* 2015). CircRNAs have been reported to be involved in the regulation of vascular smooth muscle cell processes in IA. For example, decreased expression of circ_0020397 in IA may reduce VSMC proliferation by increasing miR-138 expression and decreasing KDR expression (Wang *et al.,* 2019). The cross-head box circRNA O3 (circ-Foxo3, hsa_circ_0006404), encoded by the human *FOXO3* gene, is one of the most studied circRNAs and acts as a sponge for potential microRNAs (miRNAs). A study has clarified FOXO3 is involved in the regulation of many vascular diseases. For example, miR-30c-5p represses NLRP3 inflammasome-mediated endothelial cell apoptosis in atherosclerosis by down-regulating FOXO3 (Li *et al.,* 2018). MiR-629 regulates hypoxic pulmonary vascular remodeling by targeting FOXO3 and PERP (Zhao *et al.,* 2019). However, circ_FOXO3 in IA has not been fully studied. In recent years, research on IA has also focused on the regulation of miRNAs, which are endogenous 23 nt ncRNAs and negatively regulate gene expression. MiRNAs exert post-transcriptional functions mainly by directly binding to complementary messenger RNA and repressing the expression of target genes (Lewis *et al.,* 2005; Lynam-Lennon *et al.,* 2009; Bartel *et al.,* 2009). Dysregulation of miRNA is associated with a variety of diseases, and more and more evidence indicates that miRNAs play a momentous role in vascular diseases. For example, miR-4735-3p regulates the phenotypic regulation of VSMC by targeting HIF-1-mediated IA autophagy (Gao *et al.,* 2019). The down-regulation of MiR-29b induces the phenotypic regulation of VSMC, and its importance in the formation and progression of IA rupture is manifested (Sun *et al.,* 2017), etc. Few studies have been conducted on miR-122-5p, and the action mechanism of miR-122-5p in IA needs to be further explored. The study confirmed that circ_FOXO3

repressed $H_2O_2$-induced proliferation and accelerated apoptosis of human cerebrovascular smooth muscle cells (HBVSMC). Further mechanistic studies manifested this role of circ_FOXO3 was realized by regulating the miR-122-5p/KLF6 axis, confirming the novel mechanism of circ_FOXO3 in IA process.

## MATERIALS AND METHODS

### Research objects

Thirty-eight IA patients (the IA group) with imaging diagnosis and neurosurgical clippings from the Suzhou Hospital of Anhui Medical University, Department of Neurosurgery, Suzhou Hospital of Anhui Medical University were selected as experimental subjects. Meanwhile, temporal polar temporal cortical artery tissue was removed from 38 patients (the control group) with temporal lobe epilepsy caused by amygdala and hippocampal sclerosis and was normal arterial tissue with postoperative histopathological examination. No obvious difference was presented in gender with age in the IA and the control. Venous blood (2 tubes) was taken from all subjects on an empty stomach simultaneously in the morning prior to surgery. The approval of the research was obtained through the Institutional Review Committee of the Suzhou Hospital of Anhui Medical University, following the principles of *the Declaration of Helsinki*. Written informed consent was obtained from the participants in the investigation.

### Enzyme-linked immunosorbent assay (ELISA)

The examination of serum-related indicators was performed using an ELISA kit (NanJing JianCheng Institute of Bioengineering, Nanjing, China). After centrifugation of the blood samples, the examination of endothelin-1 (ET-1) and vascular hematoma factor (vWF) was based on the kit instructions.

### Cell culture

HBVSMC (Cat. No. CP-H116) were purchased from Procell (Wuhan, China) and grown in a humidified incubator (Roewe Instrument Co., Ltd. Shanghai, China) at 37°C with 5% $CO_2$. Dulbecco's modified eagle medium containing 10% fetal bovine serum (FBS), 100 mg/L gentamicin and 2 mmol/L glutamine were applied. To establish IA *in vitro* (Shi *et al*., 2019; Zhao et al.,2018), cells were incubated with 0, 30, 90, or 180 μM $H_2O_2$ (Sigma, St. Louis, MO, USA) for 6 h.

### 3-(4,5-dimethylthiazol-2-yl)-2,5-diphenyltetrazolium bromide (MTT) assay

Culture medium consisting of 10% serum was adopted for the preparation of a single cell suspension; The $5\times10^3$ cells per well were seeded in a 96-well plate. After separate transfection of cells with circ_FOXO3 and NC for 0, 24, and 48 h, incubation was carried out with 10 μL per well 5 mg/ml MTT. After removing the supernatant, cells were added with 100 μL dimethyl sulfoxide (DMSO, Beyotime, Shanghai, China) was present. Finally, the detection of the absorbance value was carried out using a microplate reader (Thermo Labsystems) with wavelength of 570 nm.

### Cell colony assay

The application of cells in logarithmic growth phase was for the preparation of a dispersed single cell suspension and the culture in a six-well plate medium was with 10% FBS. After removing the culture medium and transfection of the cells with circ_FOXO3 and NC, the culture medium was replaced with a new one and continued culture was conducted. Finally, after discarding the supernatant, the suspension was fixed with 4% paraformaldehyde and then stained with 0.1% crystal violet to count colonies.

### Real-time polymerase chain reaction (Rt-PCR)

The application of Trizol RNAiso (Takara) was for the extraction of total cellular RNA, and Thermo Nano Drop 2000 was used to detect the concentration and purity of total RNA, and Agilent-2100 sulfate polyacrylamide gel electrophoresis was applied to detect the integrity of total RNA. RNA was retrotranscribed to cDNA using the M-MLV reverse transcriptase kit (Thermo Fisher Scientific), and the final adoption of the quantitative real-time PCR kit was for fluorescence quantification (Takara, Japan). Primers were constructed and synthesized *via* Beijing Kinco. The adoption of GAPDH and U6 was performed as internal controls. Primer sequences were manifested in the following:

Circ_FOXO3:
- Forward primer: 5'-GGCCTCATCTCAAAGCTGG-3',
- Reverse primer: 5'-CTTGCCCGTGCCTTCATT-3';

MiR-122-5p:
- Forward primer: 5'-ACACTCCAGCTGGGAA-3',
- Reverse primer: 5'-GTGCAGGGTCCGAGGT-3'.

KLF6:
- Forward primer: 5'-GGCCAAGTTTACCTCCGACC-3',
- Reverse primer: 5'-TAAGGCTTTTCTCCTTCCCTGG-3'.

GAPDH:
- Forward primer: 5'-TTCTTTTGCGTCGCCAGGTG-3',
- Reverse primer: 5'-GGAGGGAGAGAACAGTGAGC-3'.

U6:
- Forward primer: 5'-CTCGCTTCGGCAGCACA-3',
- Reverse primer: 5'-AACGCTTCACGAATTTGCGT-3'.

### Luciferase report assay

The subclone of the circ_FOXO3 sequence or the 3'untranslated region (UTR) fragment of KLF6 containing the forecast binding site of miR-122-5p was included in the pmirglol-Luciferase target expression vector. After construction of the wild-type carriers circ_FOXO3 (pmirglol – circ_FOXO3-WT) and wild-type carriers KLF63 3'UTR (pmirglo-KLF63 3'UTR-WT) carriers, and plasmids pmirglo- KLF63 3'UTR-MUT or pmirGLO-circ_FOXO3- MUT, HBVSMC transfection was with KLF6 or circ_FOXO3 WT, MUT vectors, and miR-122-5p mimic or its NC for detection of luciferase activity via the dual luciferase Assay Kit (Promega, Madison, WI, USA).

### RNA-pull down

For verification of the binding of miR-122-5p with circ_FOXO3, the assay was conducted. After the design of 3 biotin-labeled miRNA sequences (Bio-miR-122-5p-WT, -MUT, Bio-miR-NC, GenePharma, Shanghai, China), transfection was with biotinylated oligonucleotides and then specific lysate products (Ambion, Austin, Texas, USA). After incubation of the dissolved products with m-280 plates, RNase-free streptomycin beads and yeast tRNA (from σ), the wash was with a cold solution, low- and high-salt buffer. The antagonistic miR-122-5p probe was as NC. After Trizol extracted total RNA, detection of circ_FOXO3 enrichment was by Rt-PCR.

### RNA immunoprecipitation (RIP) assay

A Magna RIPTM RNA-binding protein immunoprecipitation kit (Sigma) was used for RIP analysis. Briefly, HBVSMC lysates were incubated with magnetic beads coated with anti-Ago2 or anti- immunoglobulin G. The measurement of KLF6 and miR-122-5p enriched in the beads was done by Rt-PCR.

### Western blot

The cell protein extraction was carried out using radio-immunoprecipitation assay lysis buffer consisting of 1 mM phenylmethylsulfonyl fluoridenone with the appropriate volume. Subsequently, the application of bicinchoninic acid (Beyotime) was applied to draw a standard curve to determine protein concentration. The protein separation was performed through 10% polyacrylamide gel, electroblotting was performed onto a polyvinylidene fluoride membrane, and then block with 5% skim milk powder was implemented. After incubation with primary antibody, secondary antibody labeled with horseradish peroxidase (1:10 000; ab6721; Abcam), final conduction of the strong chemiluminescence method was for quantification (ChemiDoc-It415 Imager, upland), and Image J software was applied for quantitative analysis. Primary antibody KLF6 (1:1000; sc-365633; Santa Cruz Biotechnology) was conducted.

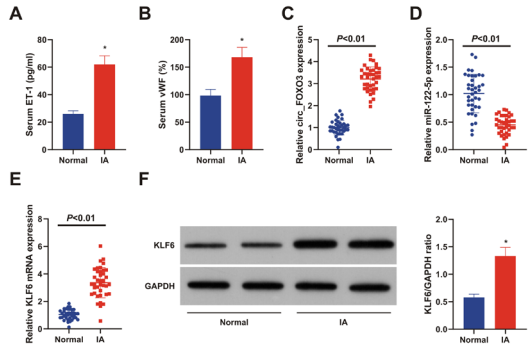


**Figure 1. Elevated circ_FOXO3 and KLF6, and reduced miR-122-5p are manifested in IA tissue**
(**A/B**) ELISA to detect ET-1 and vWF in serum from patients with IA and temporal lobe epilepsy. (**C–F**) Rt-PCR and Western blot to determine circ_FOXO3, miR-122-5p and KLF6 in IA and normal arterial tissues; n=38. The expression of the measurement data was as the means ± standard. The independent sample *t*-test was applied for comparison between groups.

### Statistical analysis

The adoption of SPSS 22.0 was for statistical analysis of the data and the expression of the results was by mean ± standard deviation. Conduction of sample comparison between two groups and multiple groups was done by independent sample t test as well as ANOVA analysis of variance. For $P<0.05$, differences was considered as statistically significant.

## RESULTS

### Strengthening circ_FOXO3 and KLF6 and reduced miR-122-5p are testified in IA tissue

Detection of factors in IA and the control manifested the elevation of ET-1, vWF, circ_FOXO3, and KLF6, and the repression of miR-122-5p in IA (Fig. 1A–F).

**Table 1. Relation of circ_FOXO3 expression with the clinicopathologic features in IA patients**

| Clinicopathological data | n | Circ_FOXO3 | | *P* |
|---|---|---|---|---|
| | | Reduced (n=25) | Elevated (n=13) | |
| Age (years) | | | | 0.694 |
| 50 or less | 10 | 6 | 4 | |
| More than 50 | 28 | 20 | 8 | |
| Gender | | | | 0.307 |
| Male | 18 | 10 | 8 | |
| Female | 20 | 15 | 5 | |
| Hunt-Hess grade | | | | 0.005 |
| I/II | 24 | 20 | 4 | |
| IIII/IV | 14 | 5 | 9 | |
| Degree of endothelial damage | | | | 0.028 |
| 0–2 | 13 | 5 | 8 | |
| 3–4 | 25 | 20 | 5 | |
| Smoking history | | | | 0.024 |
| Smoking | 27 | 21 | 6 | |
| Non-smoking | 11 | 4 | 7 | |

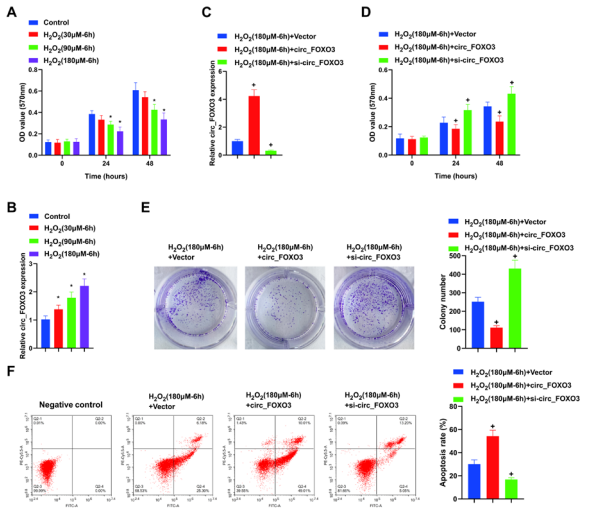

**Figure 2. Repressive circ_FOXO3 can reduce H2O2-induced HBVSMC damage**
(**A**) MTT detection of cell proliferation of HBVSMC stimulated or not stimulated with different doses of $H_2O_2$. (**B**) Rt-PCR detection of the abundance of circ_FOXO3 in HBVSMC treated with different doses of $H_2O_2$. (**C**) Transfection of circ_FOXO3 elevation/reduction vector; (**D, E**) MTT method and detection by plate cloning of HBVSMC cell proliferation after regulation of circ_FOXO3. (**F**) Flow cytometry detection of HBVSMC apoptosis after regulation of circ_FOXO3. N=3. The expression of the measurement data was as the means ± standard . *vs. control, $P$<0.05; + *vs.* $H_2O_2$ + vector, $P$<0.05.

## Hunt-Hess grade and degree of endothelial injury with smoking history were implicated in circ_FOXO3 in IA tissue

Based on the mean expression of circ_FOXO3, the assignment of the patients was made to reduced and elevated groups. Analysis of the relationship of circ_FOXO3 expression with the clinicopathological characteristics of IA patients affirmed that Hunt-Hess grade, endothelial injury degree with smoking history were involved in circ_FOXO3 ($P$<0.05), while age, sex with operation method had no correlation with circ_FOXO3 expression.

## Repressive circ_FOXO3 attenuates $H_2O_2$-induced HBVSMC damage

For analysis of the participation of circ_FOXO3 in IA, HBVSMC were applied to establish the $H_2O_2$-induced cell model. As manifested in Fig. 2A, $H_2O_2$ stimulation apparently reduced cell proliferation dose-dependently, suggesting that the *in vitro* model was successfully established. Furthermore, it was found that the abundance of circ_FOXO3 in HBVSMC was obviously elevated after $H_2O_2$ treatment (Fig. 2C). For further exploration of the character of circ_FOXO3 in the $H_2O_2$ induction model, the introduction of HBVSMC was with transfection vectors or elevation/depression vectors of circ_FOXO3 before $H_2O_2$ stimulation (Fig. 2D). It was clarified that repressive circ_FOXO3 alleviated $H_2O_2$-induced cell proliferation reduction (Fig. 2E, F) and $H_2O_2$-induced apoptosis of HBVSMC (Fig. 2G), while strengthening circ_FOXO3 was the opposite. Briefly, knockout circ_FOXO3 reduces $H_2O_2$-induced HBVSMC damage.

## MiR-122-5p combines with circ_FOXO3

Via online analysis software was predicted the specific binding region of circ_FOXO3 with miR-122-5p

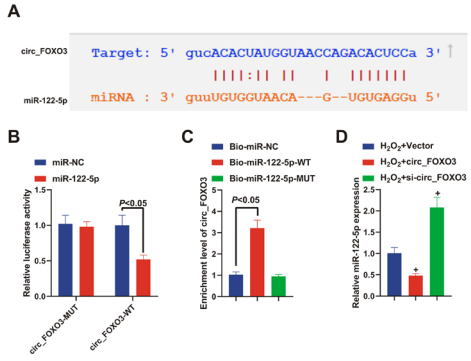

**Figure 3. MiR-122-5p binds to circ_FOXO3**
(**A**) Prediction of the bioinformatics website of binding sites of the circ_FOXO3 and miR-122-5p. (**B**) Verification of the dual luciferase reporter assay of the regulatory relationship between circ_FOXO3 and miR-122-5p. (**C**) Verification of the RNA pulldown assay of the binding relationship between circ_FOXO3 and miR-122-5p. (**D**) qPCR detection of miR-122-5p expression after regulating circ_FOXO3. N=3, and the measurement data were expressed as the means ± standard deviation. + *vs.* $H_2O_2$ + vector, $P$<0.05.

(Fig. 3A). The impairment of luciferase activity in the circ_FOXO3-WT + miR-122-5p mimic was clarified. However, no apparent difference in luciferase activity was observed in the circ_FOXO3-MUT + miR-122-5p mimic, indicating that miR-122-5p specifically binds to circ_FOXO3 (Fig. 3B). The results affirmed that *vs* Bio-miR-NC, the enrichment of circ_FOXO3 in Bio-miR-122-5p-WT was strengthened and not clearly different in Bio-miR-122-5p-MUT (Fig. 3C). Moreover, detection of miR-122-5p was conducted in the $H_2O_2$-induced cell model after the regulation of circ_FOXO3. It was found that up-regulation of circ_FOXO3 reduced miR-122-5p, while the decrease in circ_FOXO3 was contrast (Fig. 3D).

## MiR-122-5p mitigates $H_2O_2$-induced HBVSMC damage

For the study of the miR-122-5p characters in HBVSMC damage, NC, miR-122-5p, and in-miR-122-5p were transfected before exposure to $H_2O_2$ exposure (Fig. 4A). A series of assays testified that elevated miR-122-5p facilitated $H_2O_2$-induced cell proliferation (Fig. 4B, C) and decreased apoptosis (Fig. 4D), while reduced miR-122-5p was opposite. In the short term, miR-122-5p is available to attenuate $H_2O_2$-induced HBVSMC damage.

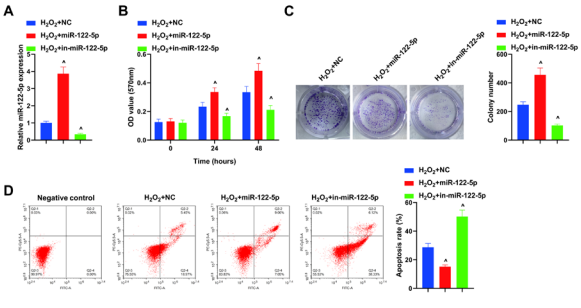

**Figure 4. MiR-122-5p attenuates H2O2-induced HBVSMC damage**
(**A**) The abundance of miR-122-5p detected in HBVSMC transfected with elevated/reduced miR-122-5p vectors. (**B–C**) MTT or plate cloning detection of HBVSMC cell proliferation transfected with miR-122-5p elevated/reduced vector. (**D**) Flow cytometry detection of apoptosis of HBVSMC transfected with miR-122-5p elevated/reduced vector. N=3. The expression of the measurement data was as the means mean ± standard . + *vs* $H_2O_2$ + NC, $P$<0.05.

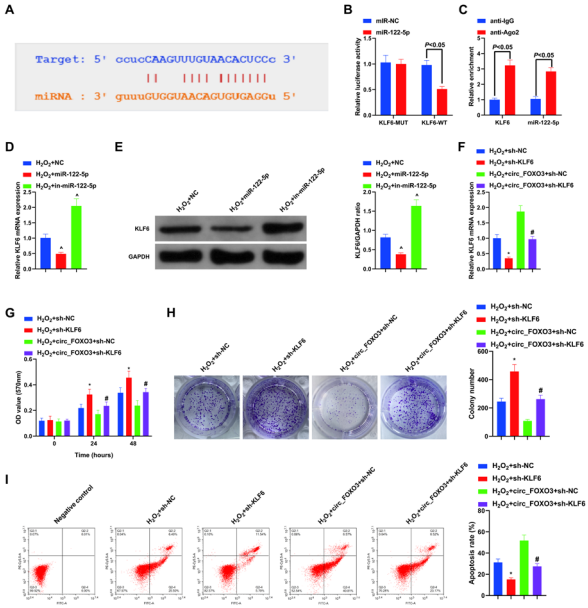

**Figure 5. KLF6 is a target of miR-122-5p and mediates the circ_FOXO3/miR-122-5p axis**
(**A**) The starBase to predict the binding sequence of miR-122-5p to KLF6. (**B**) After transfection of miR-NC or miR-122-5p, the luciferase activity of the KLF6-WT and KLF6-MUT vectors detected in HBVSMC. (**C**) The enrichment of KLF6 and miR-122-5p detected after Ago2 RIP. (**D–E**) Detection of KLF6 in HBVSMC transfected with miR-NC, miR-122-5p mimic, and miR-122-5p. (**F**) qPCR detection of transfection efficiency. (**G–H**) MTT or plate cloning detection of HBVSMC cell proliferation. (**I**) Flow cytometry detection of apoptosis of HBVSMC. N=3. The expression of the measurement data was as the means ± standard . * *vs* $H_2O_2$ + sh-NC, $P<0.05$; # *vs* $H_2O_2$ + circ_FOXO3 + sh-NC, $P<0.05$.

### MiR-122-5p targets KLF6 that mediates the modulation of the circ_FOXO3/miR-122-5p axis

For further exploration of the regulatory network of miR-122-5p, the analysis of miR-122-5p's molecular targets was carried out through starBase. KLF6 is a latent target, and the targeting of miR-122-5p on KLF6 was affirmed in Fig. 5A. For confirmation of this association, the construction of KLF6-WT and -MUT carriers was manifested. MiR-122-5p mimic resulted in an apparent reduction in luciferase activity in KLF6-WT, with no influence on the activity of KLF6-MUT (Fig. 5B). The enrichment of a large amount of KLF6 and miR-122-5p was manifested in the $AgO_2$-based complex (Fig. 5C). Furthermore, the determination of the impacts of miR-122-5p on KLF6 was made in HBVSMC introduced with miR-NC, miR-122-5p mimic and in-miR-122-5p. Elevated miR-122-5p apparently decreased KLF6, but the knockdown one was the opposite (Fig. 5D, E). Transfection of the depressive KLF6 vector and the circ_FOXO3 + sh-KLF6 vector was carried out in the $H_2O_2$-induced HBVSMC model, and validation was carried out by qPCR (Fig. 5F). In the experiment (Fig. 5G–I) that sh-KLF6 clearly facilitated cell proliferation activity, reduced the rate of apoptosis, and effectively reversed inhibition of cell proliferation and the promotion of apoptosis via elevated circ_FOXO3. Shortly, KLF6 mediates circ_FOXO3/miR-122-5p axis to regulate $H_2O_2$-induced HBVSMC damage.

## DISCUSSION

IA, named cerebral aneurysm, is a severe cerebrovascular disease resulting from weakness of the cerebral vein or artery wall (Wang *et al.,* 2019; Jin *et al.,* 2019). As neuroimaging technology develops and noninvasive screening methods emerge, such as craniocerebral angiography (CTA) and magnetic resonance angiography (MRA), elevated unruptured IA has been detected. Once IA ruptures, it will make for subarachnoid hemorrhage (SAH), with a surprising fatality rate (Kalaria *et al.,* 2002; Li *et al.,* 2013). Except for surgical cutting or interventional embolization, there is no effective medical treatment. As a new-type gene expression regulator, circRNA has also been confirmed to function pivotally in many diseases. A previous study has confirmed that endogenous competitive RNA networks related to circRNA are involved in IA development (Qin *et al.,* 2021), while functional polymorphisms in miRNA gene promoter regions have been documented to be associated with IA risk (Sima *et al.,* 2017). In this research, clinical data showed that circ_FOXO3 and KLF6 were up-regulated and miR-122-5p was down-regulated in IA tissues, and circ_FOXO3 expression was associated with Hunt-Hess grade, degree of endothelial injury, and smoking history.

As a vital cell type forming medium in intracranial arteries, smooth muscle cells are crucial in the formation and rupture of IA (Starke *et al.,* 2014). With reference to previous studies (Wang *et al.,* 2018), circRNAs are associated with VSMC dysfunction and the presence of IA (Huang *et al.,* 2019). Circ_FOXO3 is a promising cancer-related biomarker (Yang et al., 2021), in bladder cancer (Li *et al.,* 2020) and squamous cell carcinoma of the esophagus (Xing *et al.,* 2020). In this study, transfection of elevated or reduced circ_FOXO3 vectors into the $H_2O_2$-stimulated HBVSMC model found that suppressive circ_FOXO3 could promote $H_2O_2$-induced HBVSMC cell proliferation and inhibit apoptosis, while overexpressed circ_FOXO3 could do the opposite. It was suggested that knockdown circ_FOXO3 can attenuate H2O2-induced HBVSMC damage.

Next, the regulatory mechanism downstream of circ_FOXO3 was explored. The binding site of circ_FOXO3 with miR-122-5p was predicted through bioinformatics websites, which was verified. Previous studies manifested that miR-122-5p was involved in the regulation of various cells, such as breast cancer (Huang *et al.,* 2021), cervical cancer (Gao *et al.,* 2021), etc. It was confirmed in the study the proliferation-promoting and antiapoptotic effects of miR-122-5p in HBVSMC introduced with $H_2O_2$, while the reduction of miR-122-5p was the contrary. The above experiments confirmed that circ_FOXO3 aggravated $H_2O_2$-induced HBVSMC damage by repressing miR-122-5p.

Next, further exploration was carried out at the downstream target of miR-122-5p. KLF6, a member of the specific protein 1/Krupel-like transcription factor family (Sp1/KLF), is originally cloned from white blood cells. KLF6 is obviously increased in VSMC of diabetic patients and in VSMC treated with high glucose (Zhou *et al.,* 2020). In the results, KLF6 was recognized as a functional target of miR-122-5p. Furthermore, curbed KLF6 apparently increased cell proliferation and reduced apoptosis. Furthermore, by cotransfection of KLF6 with circ_FOXO3, repressive KLF6 reversed the up-regulated damage of circ_FOXO3 to $H_2O_2$-treated HBVSMCs, suggesting that KLF6 is involved in mediating circ_FOXO3.

In summary, the study found that circ_FOXO3 can facilitate the proliferation and induce $H_2O_2$-induced HB-VSMC apoptosis, which was achieved by regulating miR-122-5p with KLF6 targeting. Later animal models of IA will be applied for further *in vivo* analysis.

## Declarations

**Acknowledgements.** Not applicable.
**Funding Statements.** Not applicable.
**Declaration of Conflicting Interests.** The author(s) declared no potential conflicts of interest with respect to the research, authorship, and/or publication of this article.

## REFERENCE

Bartel DP (2009) MicroRNAs: target recognition and regulatory functions. *Cell* **136**: 215–233. https://doi.org/10.1016/j.cell.2009.01.002
Chen LL, Yang L (2015) Regulation of circRNA biogenesis. *RNA Biol* **12**: 381–388. https://doi.org/10.1080/15476286.2015.1020271
El Rouby S, Newcomb EW (1996) Identification of Bcd, a novel proto-oncogene expressed in B-cells. *Oncogene* **13**: 2623–2630. PMID: 9000136
Etminan N, Rinkel GJ (2016) Unruptured intracranial aneurysms: development, rupture and preventive management. *Nat Rev Neurol* **12**: 699–713. https://doi.org/10.1038/nrneurol.2016.150
Frösen J, Joutel A (2018) Smooth muscle cells of intracranial vessels: from development to disease. *Cardiovasc Res* **114**: 501–512. https://doi.org/10.1093/cvr/cvy002
Gao G, Zhang Y, Chao Y, Niu C, Fu X, Wei J (2019) miR-4735-3p regulates phenotypic modulation of vascular smooth muscle cells by targeting HIF-1-mediated autophagy in intracranial aneurysm. *J Cell Biochem* **120**: 19432–19441. https://doi.org/10.1002/jcb.29219
Gao Z, Wang Q, Ji M, Guo X, Li L, Su X (2021) Exosomal lncRNA UCA1 modulates cervical cancer stem cell self-renewal and differentiation through microRNA-122-5p/SOX2 axis. *J Transl Med* **19**: 229. https://doi.org/10.1186/s12967-021-02872-9
Huang, Q., Huang, Q.Y., Sun, Y. & Wu, S. (2019) High-throughput data reveals novel circular rnas *via* competitive endogenous rna networks associated with human intracranial aneurysms. *Med Sci Monit* **25**: 4819–4830. https://doi: 10.12659/msm.917081. **Retracted Publication, please delete from text**
Huang X, Luo Y, Li X (2022) Circ_0072995 Promotes ovarian cancer progression through regulating miR-122-5p/SLC1A5 axis. *Biochem Genet* **60**: 153–172. https://doi.org/10.1007/s10528-021-10092-5
Jin D, Song C, Leng X, Han P (2019) A systematic review and meta-analysis of risk factors for unruptured intracranial aneurysm growth. *Int J Surg* **69**: 68–76. https://doi.org/10.1016/j.ijsu.2019.07.023
Kalaria RN, Kalimo H (2002) Introduction: Non-atherosclerotic cerebrovascular disorders. *Brain Pathol* **12**: 337–342. https://doi.org/10.1111/j.1750-3639.2002.tb00448.x
Lewis BP, Burge CB, Bartel DP (2005) Conserved seed pairing, often flanked by adenosines, indicates that thousands of human genes are microRNA targets. *Cell* **120**: 15–20. https://doi.org/10.1016/j.cell.2004.12.035
Li MH, Chen SW, Li YD, Chen YC, Cheng YS, Hu DJ, Tan HQ, Wu Q, Wang W, Sun ZK, Wei XE, Zhang JY, Qiao RH, Zong WH, Zhang Y, Lou W, Chen ZY, Zhu Y, Peng DR, Ding SX, Xu XF, Hou XH, Jia WP (2013) Prevalence of unruptured cerebral aneurysms in Chinese adults aged 35 to 75 years: a cross-sectional study. *Ann Intern Med* **159**: 514–521. https://doi.org/10.7326/0003-4819-159-8-201310150-00004
Li P, Zhong X, Li J, Liu H, Ma X, He R, Zhao Y (2018) MicroRNA-30c-5p inhibits NLRP3 inflammasome-mediated endothelial cell pyroptosis through FOXO3 down-regulation in atherosclerosis. *Biochem Biophys Res Commun* **503**: 2833–2840. https://doi.org/10.1016/j.bbrc.2018.08.049
Li, Y., Qiao, L., Zang, Y., Ni, W. & Xu, Z. (2020) Circular RNA FOXO3 suppresses bladder cancer progression and metastasis by regulating MiR-9-5p/TGFBR2. *Cancer Manag Res* **12**: 5049–5056. https://doi: 10.2147/cmar.S253412. **Retracted paper, please delete from text**
Liu Z, Ajimu K, Yalikun N, Zheng Y, Xu F (2019) Potential therapeutic strategies for intracranial aneurysms targeting aneurysm pathogenesis. *Front Neurosci* **13**: 1238. https://doi.org/10.3389/fnins.2019.01238
Lynam-Lennon N, Maher SG, Reynolds JV (2009) The roles of microRNA in cancer and apoptosis. *Biol Rev Camb Philos Soc* **84**: 55–71. https://doi.org/10.1111/j.1469-185X.2008.00061.x
Mandelbaum M, Kolega J, Dolan JM, Siddiqui AH, Meng H (2013) A critical role for proinflammatory behavior of smooth muscle cells in hemodynamic initiation of intracranial aneurysm. *PLoS One* **8**: e74357. https://doi.org/10.1371/journal.pone.0074357
Maumus-Robert S, Debette S, Bérard X, Mansiaux Y, Tubert-Bitter P, Pariente A (2020) Risk of intracranial aneurysm and dissection and fluoroquinolone use: a case-time-control study. *Stroke* **51**: 994–997. https://doi.org/10.1161/strokeaha.119.028490
Qin K, Tian G, Zhou D, Chen G (2021) Circular RNA circ-ARFIP2 regulates proliferation, migration and invasion in human vascular smooth muscle cells *via* miR-338-3p-dependent modulation of KDR. *Metab Brain Dis* **36**: 1277–1288. https://doi.org/10.1007/s11011-021-00726-3
Salzman J, Gawad C, Wang PL, Lacayo N, Brown PO (2012) Circular RNAs are the predominant transcript isoform from hundreds of human genes in diverse cell types. *PLoS One* **7**: e30733. https://doi.org/10.1371/journal.pone.0030733
Shi Y, Li S, Song Y, Liu P, Yang Z, Liu Y, Quan K, Yu G, Fan Z, Zhu W (2019) Nrf-2 signaling inhibits intracranial aneurysm formation and progression by modulating vascular smooth muscle cell phenotype and function. *J Neuroinflammation* **16**: 185. https://doi.org/10.1186/s12974-019-1568-3
Sima X, Sun H, Zhou P, You C, Cai B (2017) Association between functional polymorphisms in the promoter of the miR-143/145 cluster and risk of intracranial aneurysm. *Sci Rep* **7**: 43633. https://doi.org/10.1038/srep43633
Starke RM, Chalouhi N, Ding D, Raper DM, Mckisic MS, Owens GK, Hasan DM, Medel R, Dumont AS (2014) Vascular smooth muscle cells in cerebral aneurysm pathogenesis. *Transl Stroke Res* **5**: 338–346. https://doi.org/10.1007/s12975-013-0290-1
Sun L, Zhao M, Zhang J, Lv M, Li Y, Yang X, Liu A, Wu Z (2017) MiR-29b Downregulation induces phenotypic modulation of vascular smooth muscle cells: implication for intracranial aneurysm formation and progression to rupture. *Cell Physiol Biochem* **41**: 510–518. https://doi.org/10.1159/000456887
Wang L, Wei Y, Yan Y, Wang H, Yang J, Zheng Z, Zha J, Bo P, Tang Y, Guo X, Chen W, Zhu X, Ge L (2018) CircDOCK1 suppresses cell apoptosis via inhibition of miR-196a-5p by targeting BIRC3 in OSCC. *Oncol Rep* **39**: 951–966. https://doi.org/10.3892/or.2017.6174
Wang X, Zhu C, Leng Y, Degnan AJ, Lu J (2019) Intracranial aneurysm wall enhancement associated with aneurysm rupture: a systematic review and meta-analysis. *Acad Radiol* **26**: 664–673. https://doi.org/10.1016/j.acra.2018.05.005
Wang Y, Wang Y, Li Y, Wang B, Miao Z, Liu X, Ma Y (2019) Decreased expression of circ_0020397 in intracranial aneurysms may be contributing to decreased vascular smooth muscle cell proliferation *via* increased expression of miR-138 and subsequent decreased KDR expression. *Cell Adh Migr* **13**: 220–228. https://doi.org/10.1080/19336918.2019.1619432
Xing Y, Zha WJ, Li XM, Li H, Gao F, Ye T, Du WQ, Liu YC (2020) Circular RNA circ-Foxo3 inhibits esophageal squamous cell cancer progression *via* the miR-23a/PTEN axis. *J Cell Biochem* **121**: 2595–2605. https://doi.org/10.1002/jcb.29481
Yang T, Li Y, Zhao F, Zhou L, Jia R (2021) Circular RNA Foxo3: A promising cancer-associated biomarker. *Front Genet* **12**: 652995. https://doi.org/10.3389/fgene.2021.652995
Zhao M, Chen N, Li X, Lin L (2019) MiR-629 regulates hypoxic pulmonary vascular remodelling by targeting FOXO3 and PERP. *J Cell Mol Med* **23**: 5165–5175. https://doi.org/10.1111/jcmm.14385
Zhao W, Zhang H, Su JY (2018) MicroRNA-29a contributes to intracranial aneurysm by regulating the mitochondrial apoptotic pathway. *Mol Med Rep* **18**: 2945–2954. https://doi.org/10.3892/mmr.2018.9257
Zhou J, Zhang L, Zheng B, Zhang L, Qin Y, Zhang X, Yang Z, Nie Z, Yang G, Yu J, Wen J (2020) *Salvia miltiorrhiza* bunge exerts antioxidative effects through inhibiting KLF10 expression in vascular smooth muscle cells exposed to high glucose. *J Ethnopharmacol* **262**: 113208. https://doi.org/10.1016/j.jep.2020.113208